

Preparation and characteristics of $\text{Ba}_{0.5}\text{Sr}_{0.5}\text{Co}_{0.8}\text{Fe}_{0.2}\text{O}_{3-\delta}$ cathodes for IT-SOFCs by electrostatic slurry spray deposition

Jinyi Choi^a, Jongmo Im^b, Inyu Park^a, Dongwook Shin^{a,b,*}

^aDepartment of Fuel Cells and Hydrogen Technology, Hanyang University, 17 Haengdang-dong, Seongdong-gu, Seoul 133-791, Republic of Korea

^bDivision of Materials Science & Engineering, Hanyang University, 17 Haengdang-dong, Seongdong-gu, Seoul 133-791, Republic of Korea

Available online 24 May 2011

Abstract

To solve the interfacial peeling-off problem of cathode materials $\text{Ba}_{0.5}\text{Sr}_{0.5}\text{Co}_{0.8}\text{Fe}_{0.2}\text{O}_{3-\delta}$ (BSCF), electrostatic slurry spray deposition (ESSD) was applied. The BSCF cathode was deposited on a CGO pellet by ESSD and the electrochemical performance of the BSCF cathode is investigated at various temperatures (650–800 °C) and oxygen partial pressures (0.15–0.8 atm). Microstructural observation showed that the BSCF/CGO half cell exhibited good adhesion between cathode and electrolyte layers without any cracks for peeling-off problem. The polarization resistance was estimated to $1.78 \Omega \text{ cm}^2$ at 650 °C and the average activation energy was $118.8 \text{ kJ mol}^{-1}$. The dependence of polarization resistances on Po_2 shows that the rate-determining step of the oxygen reduction reaction in the prepared BSCF cathode is the charge transfer between electrolyte and electrode.

© 2011 Elsevier Ltd and Techna Group S.r.l. All rights reserved.

Keywords: C. Thermal expansion; D. Perovskites; SOFCs; BSCF

1. Introduction

Lowering operation temperature is one of the efforts to mitigate the major problems originating from the high temperature operation of solid oxide fuel cells (SOFCs). In anode-supported SOFCs, the cathode polarization resistance is the major contribution to the total loss in a cell and for intermediate temperature operation this becomes more serious. Therefore, it is important to choose the suitable cathode materials for maintaining the cell performance below 800 °C.

Compared with the perovskite-type manganites based materials such as LSM [1], perovskite related cobaltites possess considerably better cathodic and transport properties [2]. Among the cobaltite mixed ionic and electronic conductor (MIEC), $\text{Ba}_{0.5}\text{Sr}_{0.5}\text{Co}_{0.8}\text{Fe}_{0.2}\text{O}_{3-\delta}$ (BSCF) has received considerable attention as a cathode material for IT-SOFCs offering excellent performances attributed to the high rate of oxygen diffusion through the material [3,4]. Although the BSCF has good

performance, the thermal expansion coefficient (TEC) of BSCF is extraordinary high [5]. The large thermal expansion becomes a critical problem as a cathode since it causes the detachment at the interface, and results in poor electrical contact. Lim et al. reported that peeling-off phenomena were observed in various compositions of pure BSCF cathode [4]. Thus, the improvement in the fabrication method for reducing the mismatch could be one of the viable approaches. Electrostatic slurry spray deposition (ESSD), developed by author's group, utilizes electrostatic spraying of slurries containing powders and organic additives for slurry stabilization and rheological control. It has several advantages over the general electrostatic spray deposition (ESD) using precursor solution, e.g., high deposition rate, the stability of the crystal phase, much less formation of crack and better adhesion to substrate caused by deposition condition at room temperature. The highly charged slurry droplets in the ESSD can be as small as particle size of raw powder and, thus, the shrinkage during the sintering process will be minimized. Therefore it is expected that this method possesses more freedom to design the microstructure compared to conventional screen printing process.

In the present work, by employing the aforementioned ESSD, we successfully fabricated pure $\text{Ba}_{0.5}\text{Sr}_{0.5}\text{Co}_{0.8}\text{Fe}_{0.2}\text{O}_{3-\delta}$

* Corresponding author at: Department of Fuel Cells and Hydrogen Technology, Hanyang University, 17 Haengdang-dong, Seongdong-gu, Seoul 133-791, Republic of Korea. Tel.: +82 2 2220 0503; fax: +82 2 2220 4011.

E-mail address: dwshin@hanyang.ac.kr (D. Shin).

cathodes on $\text{Gd}_{0.2}\text{Ce}_{0.8}\text{O}_{1.9}$ electrolyte without any detachment by the ESSD method. Chemical compatibility and microstructure were studied and electrochemical performance at intermediate temperature (650–800 °C) was analyzed.

2. Experimental

Dense pellet of $\text{Gd}_{0.2}\text{Ce}_{0.8}\text{O}_{1.9}$ (CGO) of 21 mm in diameter and 1 mm thick was obtained by uniaxially pressing commercial CGO powder (32.8 m²/g, Nextech, USA), and then sintering at 1400 °C for 5 h in air. The $\text{Ba}_{0.5}\text{Sr}_{0.5}\text{Co}_{0.8}\text{Fe}_{0.2}\text{O}_{3-\delta}$ (BSCF) slurry was obtained by mixing commercial BSCF powders with solvents, homogenizer, and dispersant. The mixture was ball milled to break up the agglomerated particles for 48 h. The BSCF cathode layers were deposited onto the pre-sintered CGO substrates by electrostatic slurry spray deposition (ESSD) technique. After electrostatic spraying and drying in air, the cells were sintered at 950 °C for 2 h in air.

The crystal structure of the fabricated BSCF cathode layer was examined with an X-ray diffractometer (Rigaku ULTIMA IV, Japan) using monochromatic Cu K α radiation with a step size of 0.014° in a 2θ range of 20–80° generated at 40 kV and 40 mA. Characterization of the microstructure of the BSCF cathode layer was performed using scanning electron microscopy (JEOL JCM-5700, Japan). Electrochemical impedance measurements were also carried out at temperatures ranging from 650 °C to 800 °C by using a frequency response analyzer (SI 1260, UK) combined with an electrochemical interface (SI 1287, UK) in air. The oxygen partial pressure (P_{O_2}) is varied between 0.15 and 0.8 atm using oxygen/nitrogen mixture gas. Impedance spectroscopy data were collected in the frequency range of 0.1 Hz to 1 MHz with AC amplitude of 20 mV and analyzed with the Zplot/Zview software.

3. Results and discussion

Fig. 1 shows the X-ray diffraction (XRD) pattern of the BSCF cathode deposited on the CGO pellet after sintering. As can be seen, all the peaks are well indexed to the cubic perovskite structure, and sharp peaks represent a well-developed crystalline structure. No impure second phases

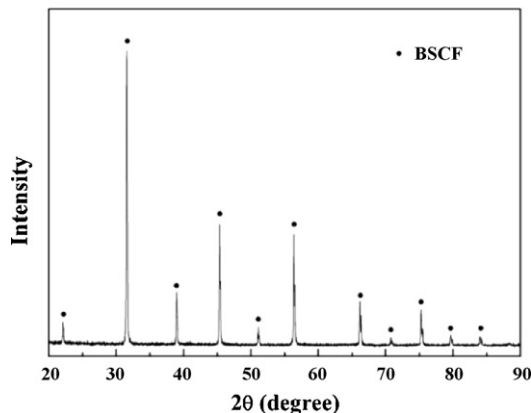


Fig. 1. The X-ray diffraction pattern of the sintered BSCF layer on CGO pellet.

were found, reflecting that the deposited BSCF cathode has a good chemical compatibility with the CGO electrolyte.

The cross-sectional micrograph in Fig. 2(a) shows that good adhesion and no distinct cracks are observed between dense CGO electrolyte and porous BSCF cathode. Uniformly porous BSCF cathode layers were formed with well developed open pore network and without any surface and interfacial cracks. The cathode thickness is about 30 μm and is controlled by changing the deposition time. The highly porous structure of cathode layer can be seen from surface image in Fig. 2(b). Sufficient porosity of ~30% was obtained when estimated by image analysis program.

As mentioned above, the sample prepared by ESSD method showed much better adhesion in contrast to previous reports, which reported that the detachment occurred between the BSCF layer and electrolyte materials fabricated by conventional method such as screen printing or tape casting. Compared with the conventional methods, the main difference of ESSD is the slurry viscosity. The screen printing and tape casting are typically used the high-viscosity slurry containing large amount of binder, while the ESSD method in this work employs the slurry of lower viscosity containing less or no binder. Salam et al. reported that the content of binder significantly affects the adhesion property with substrate in cathode layer deposited process [6]. In the screen printing and tape casting, films are formed by applying downward force and parallel motion with squeegee and blade on the high-viscosity slurry. In this process, the shrinkage occurs in vertical direction of the substrate, the thickness direction, and not on the width of the cathode layer.

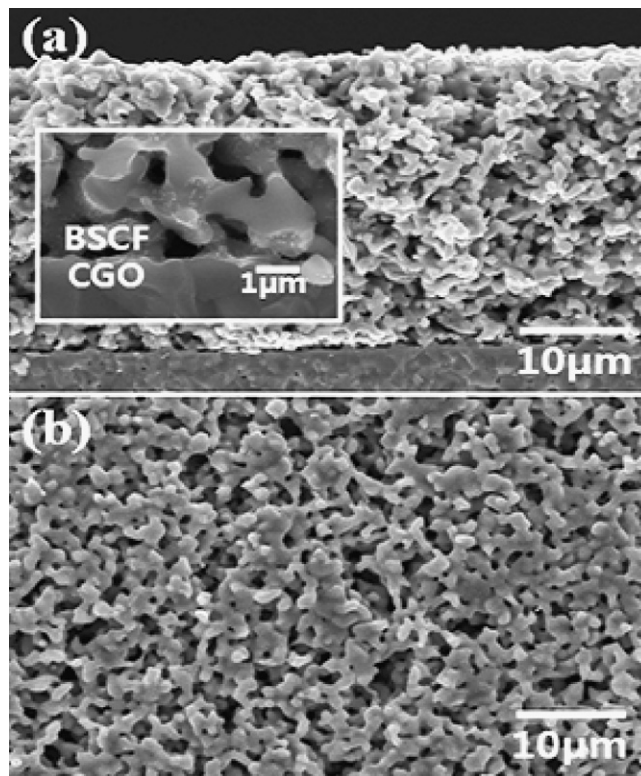


Fig. 2. SEM morphologies of (a) cross-section and (b) surface of BSCF cathode.

Also, the slurry with higher binder contents tends to have higher surface tension, leading to poorer wetting between cathode layer and electrolyte substrate. Although these phenomena are common in all types of material systems, especially for material systems with a large thermal expansion mismatch such as BSCF ($18.53 \times 10^{-6} \text{ K}^{-1}$) and CGO ($13.11 \times 10^{-6} \text{ K}^{-1}$) [7], this problem becomes more evident and will deteriorate the interfacial characteristics more seriously. However, since the ESSD process employs slurry with smaller amount solvent the better wetting and lower shrinkage are expected during the drying or heat treatment, resulting in improved adhesion between two layers.

In order to evaluate the performance of BSCF as a cathode, the impedance spectra of the as-prepared cells under open-current conditions at different temperatures from 650 to 800 °C as shown in Fig. 3(a). In these spectra, the intercept at low frequency represents the total resistance of the cell and the intercept at high frequency corresponds to electrolyte resistance. The difference of the two values is the cathode polarization resistance. The polarization resistance was estimated to 1.78 (cm^2 at 650 °C and 0.16 (cm^2 at 800 °C, respectively. The best fitting result was achieved with the equivalent circuit of $LR_{\text{e}}(R_{\text{HF}}\text{CPE})(R_{\text{LF}}\text{C})$ as shown in Fig. 3(b), indicating that at least two different electrode processes corresponding to the high and low frequency arcs are active. The series resistance, R_{e} , corresponds to the overall ohmic resistance including of the electrolyte resistance and the resistance of the lead wires. The resistance R_{HF} and R_{LF} can be attributed to the polarization resistance during the cathode reaction. Fig. 4 shows the Arrhenius plot of the cathode. The temperature dependence for the cathode was nearly linear, and the activation energy (E_{a}) calculated from the slope of linear fit is $118.8 \text{ kJ mol}^{-1}$.

Fig. 5(a) shows that the polarization resistance, R_{p} , increased from 0.85 to 1.35 (cm^2 when the oxygen partial pressure was decreased from 0.8 to 0.15 atm at 657 °C. Two arcs could be observed and fitted to CPE and C with a resistance noted R_{HF}

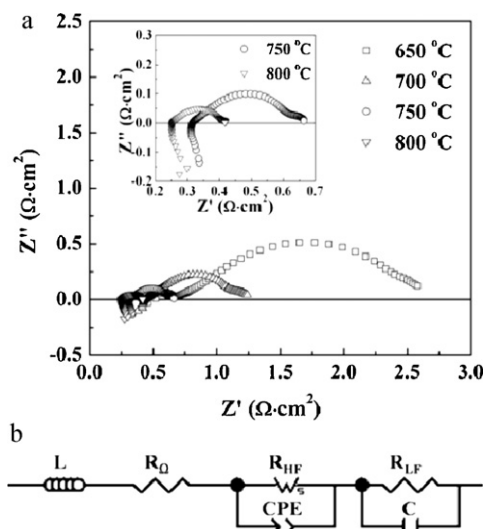


Fig. 3. (a) AC impedance spectra of the BSCF/CGO cell at different temperatures in air. (b) The equivalent circuit for fitting AC impedance spectra.

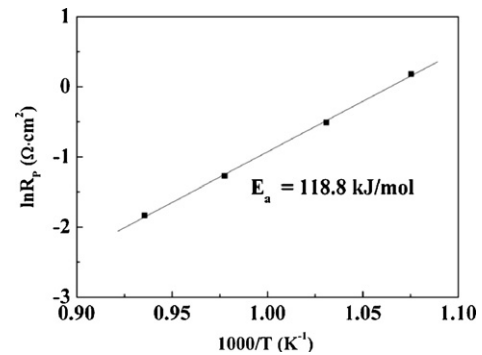


Fig. 4. Arrhenius plot of the polarization resistances measured at different temperatures.

for the high-frequency arc and R_{LF} for the low frequency arc. The polarization resistance ($R_{\text{HF}} + R_{\text{LF}}$) decreased with increasing oxygen partial pressure, obeying Eq. (1) [8]:

$$R_{\text{p}} \propto \text{Po}_2^{-n} \quad (1)$$

where R_{p} is the polarization resistance. The reaction order n gives information about the species involved in the cathode reaction.

As shown by Fig. 5(b) at 657 °C, a $\text{Po}_2^{-0.47}$ dependence was found for the low frequency arc, with a $\text{Po}_2^{-0.23}$ dependence for the high frequency resistance. A $\text{Po}_2^{-0.47}$ dependence may be attributed to a rate-determining step involving dissociation of

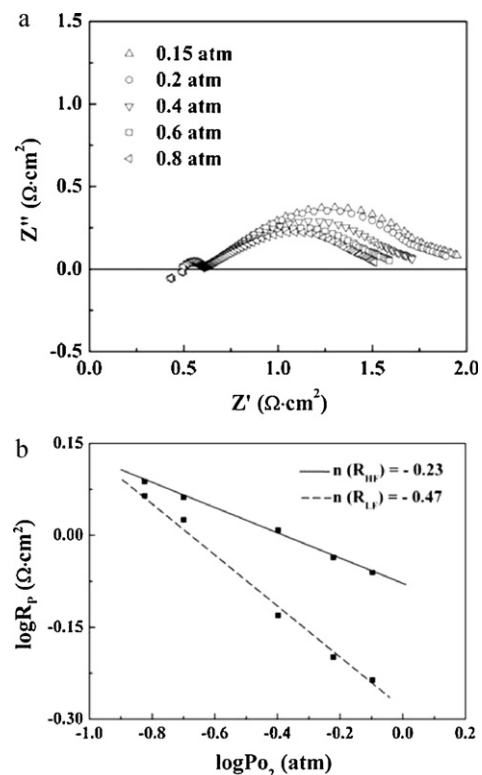


Fig. 5. (a) Impedance spectra of BSCF/CGO cell measured under different oxygen partial pressure at 657 °C. (b) $\text{Log}(R_{\text{p}})$ vs. $\text{log}(\text{Po}_2)$ plots of BSCF electrode measured at 657 °C.

molecular oxygen and atomic oxygen diffusion, while a $\text{Po}_2^{-0.23}$ dependence is attributed to oxygen ion charge transfer between electrode and electrolyte [9]. The high frequency arc is larger than the low frequency one, which indicates that the charge transfer between electrolyte and electrode is the rate-determining step through the overall reaction [8].

4. Conclusions

A porous and crack-free BSCF cathode layer is successfully obtained by electrostatic slurry spray deposition onto CGO pellet with about 30 μm thickness. The pure BSCF layer maintained good adhesion to the CGO electrolyte even after drying and sintering process. This good adhesion is believed to be due to the lower viscosity, less binder contents of slurry resulting in improved wetting and less shrinkage. The polarization resistance was estimated to 1.78 (cm^2 at 650 $^\circ\text{C}$) and the average activation energy was 118.8 kJ mol^{-1} . The impedance spectra show two depressed arcs at high and low frequencies, suggesting that there are two different processes in the cathode reaction.

From the experimental results, one can conclude that the ESSD process is very promising to solve the problem of BSCF cathode and the further optimization of the ESSD process will give us more choices for the fabrication of the cathode layers with a large TEC.

Acknowledgements

This work is the outcome of a Manpower Development Program for Energy supported by the Ministry of Knowledge

and Economy (MKE), and also supported by Solid oxide fuel cell of New & Renewable Energy R&D program (20093021030010) under the Korea Ministry of Knowledge Economy (MKE).

References

- [1] S.P. Jiang, Development of lanthanum strontium manganite perovskite cathode materials of solid oxide fuel cells: a review, *Journal of Materials Science* 43 (2008) 6799–6833.
- [2] E.V. Tsipis, V.V. Kharton, Electrode materials and reaction mechanisms in solid oxide fuel cells: a brief review, *Journal of Solid State Electrochemistry* 12 (2008) 1367–1391.
- [3] Z. Shao, S.M. Haile, A high-performance cathode for the next generation of solid-oxide fuel cells, *Nature* 431 (2004) 170.
- [4] Y.H. Lim, J. Lee, J.S. Yoon, C.E. Kim, H.J. Hwang, Electrochemical performance of $\text{Ba}_{0.5}\text{Sr}_{0.5}\text{Co}_x\text{Fe}_{1-x}\text{O}_{3-\delta}$ ($x = 0.2\text{--}0.8$) cathode on a ScSZ electrolyte for intermediate temperature SOFCs, *Journal of Power Sources* 171 (2007) 79–85.
- [5] B. Wei, Z. Lu, S. Li, Y. Liu, K. Liu, W. Su, Thermal and electrical properties of new cathode material $\text{Ba}_{0.5}\text{Sr}_{0.5}\text{Co}_{0.8}\text{Fe}_{0.2}\text{O}_{3-\delta}$ for solid oxide fuel cells, *Electrochemical and Solid-State Letters* 8 (2005) 428–431.
- [6] L.A. Salam, R.D. Matthews, H. Robertson, Optimization of thermoelectric green tape characteristics made by the tape casting method, *Materials Chemistry and Physics* 62 (2000) 263–272.
- [7] Y. Wang, S. Wang, Z. Wang, T. Wen, Z. Wen, Performance of $\text{Ba}_{0.5}\text{Sr}_{0.5}\text{Co}_{0.8}\text{Fe}_{0.2}\text{O}_{3-\delta}$ –CGO–Ag cathode for IT-SOFCs, *Journal of Power Sources* 171 (2007) 79–85.
- [8] B. Liu, Y. Zhang, L. Zhang, Oxygen reduction mechanism at $\text{Ba}_{0.5}\text{Sr}_{0.5}\text{Co}_{0.8}\text{Fe}_{0.2}\text{O}_{3-\delta}$ cathode for solid oxide fuel cell, *International Journal of Hydrogen Energy* 34 (2009) 1008–1014.
- [9] S.P. Jiang, W. Wang, Fabrication and performance of GDC-impregnated (La,Sr) MnO_3 cathodes for intermediate temperature solid oxide fuel cells, *Journal of Electrochemical Society* 152 (7) (2005) A1398–A1408.